# Hen-or-egg causality: Atmospheric $CO_2$ and temperature

Demetris Koutsoyiannis[1] and Zbigniew W. Kundzewicz[2]

[1] Department of Water Resources and Environmental Engineering, School of Civil Engineering, National Technical University of Athens, Greece (dk@itia.ntua.gr)

[2] Institute for Agricultural and Forest Environment, Polish Academy of Sciences, Poznań, Poland (kundzewicz@yahoo.com)

## Graphical abstract

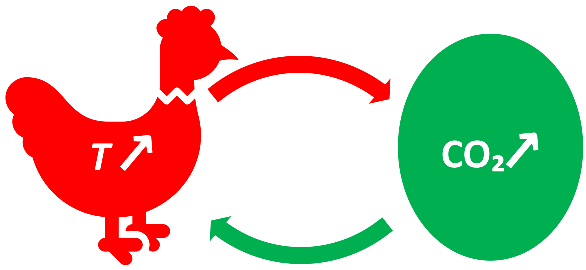


## Highlights

Relation of atmospheric $CO_2$ and temperature can be seen as a "hen-or-egg" problem.

Both causality directions exist, but the direction ($T \rightarrow CO_2$) prevails over ($CO_2 \rightarrow T$).

Changes in $CO_2$ concentration are found to follow changes in global temperature.

We interpret this postulating a biochemical mechanism in a positive feedback loop.

## Abstract

Relationships between atmospheric concentration of carbon dioxide and the global temperature are widely recognized. It is a common knowledge that increasing $CO_2$ concentration plays the major role in enhancement of the greenhouse effect and contributes to global warming. The purpose of this study is to complement the conventional and established theory that increased $CO_2$ concentration due to human emissions cause increase of temperature, by considering the reverse causality. Since increased temperature causes increase in $CO_2$ concentration, relations of atmospheric $CO_2$ and temperature may qualify into the category of "hen-or-egg" problems, where it is not always clear which of two interrelated events is the cause and which the effect. We examine the relationship of global temperature and atmospheric carbon dioxide concentration at the monthly time step, covering the time interval 1980-2019, in which reliable instrumental measurements are available. The results of our study support the hypothesis that both causality directions exist, with the direction ($T \rightarrow CO_2$) being the dominant. Changes in $CO_2$ follow changes in $T$ by about six months on monthly scale, or about one year on annual scale. We attempt to interpret this mechanism by noting the possibility of a positive feedback loop involving biochemical reactions, as soil respiration leads to increasing $CO_2$ emission at higher temperatures.

**Keywords** temperature; global warming; greenhouse gases; atmospheric $CO_2$ concentration

# Hen-or-egg causality: Atmospheric $CO_2$ and temperature

Demetris Koutsoyiannis[1] and Zbigniew W. Kundzewicz[2]

**Graphical abstract**

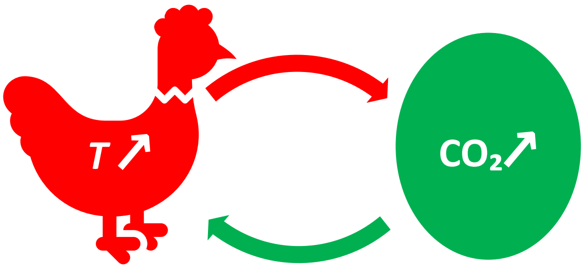

*Highlights (for review : 3 to 5 bullet points (maximum 85 characters including spaces per bullet point)

# Hen-or-egg causality: Atmospheric $CO_2$ and temperature

Demetris Koutsoyiannis[1] and Zbigniew W. Kundzewicz[2]

**Highlights**

Relation of atmospheric $CO_2$ and temperature can be seen as a “hen-or-egg” problem.

Both causality directions exist, but the direction ($T \rightarrow CO_2$) prevails over ($CO_2 \rightarrow T$).

Changes in $CO_2$ concentration are found to follow changes in global temperature.

We interpret this postulating a biochemical mechanism in a positive feedback loop.

# Hen-or-egg causality: Atmospheric $CO_2$ and temperature

Demetris Koutsoyiannis[1] and Zbigniew W. Kundzewicz[2]

[1] Department of Water Resources and Environmental Engineering, School of Civil Engineering, National Technical University of Athens, Greece (dk@itia.ntua.gr)

[2] Institute for Agricultural and Forest Environment, Polish Academy of Sciences, Poznań, Poland (kundzewicz@yahoo.com)

**Graphical abstract**

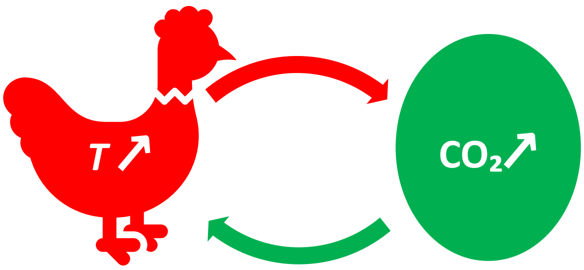


**Highlights**

Relation of atmospheric $CO_2$ and temperature can be seen as a "hen-or-egg" problem.

Both causality directions exist, but the direction ($T \rightarrow CO_2$) prevails over ($CO_2 \rightarrow T$).

Changes in $CO_2$ concentration are found to follow changes in global temperature.

We interpret this postulating a biochemical mechanism in a positive feedback loop.

**Abstract**

Relationships between atmospheric concentration of carbon dioxide and the global temperature are widely recognized. It is a common knowledge that increasing $CO_2$ concentration plays the major role in enhancement of the greenhouse effect and contributes to global warming. The purpose of this study is to complement the conventional and established theory that increased $CO_2$ concentration due to human emissions cause increase of temperature, by considering the reverse causality. Since increased temperature causes increase in $CO_2$ concentration, relations of atmospheric $CO_2$ and temperature may qualify into the category of "hen-or-egg" problems, where it is not always clear which of two interrelated events is the cause and which the effect. We examine the relationship of global temperature and atmospheric carbon dioxide concentration at the monthly time step, covering the time interval 1980-2019, in which reliable instrumental measurements are available. The results of our study support the hypothesis that both causality directions exist, with the direction ($T \rightarrow CO_2$) being the dominant. Changes in $CO_2$ follow changes in $T$ by about six months on monthly scale, or about one year on annual scale. We attempt to interpret this mechanism by noting the possibility of a positive feedback loop involving biochemical reactions, as soil respiration leads to increasing $CO_2$ emission at higher temperatures.

**Keywords** temperature; global warming; greenhouse gases; atmospheric $CO_2$ concentration

*Πότερον ἡ ὄρνις πρότερον ἢ τὸ ᾠὸν ἐγένετο* (Which of the two came first, the hen or the egg?)

Πλούταρχος, Ηθικά, Συμποσιακὰ Β, Πρόβλημα Γ (Plutarch, Moralia, Quaestiones convivales, B, Question III)

## 1 Introduction

The phrase "hen-or-egg" (also known as "chicken-or-egg" or "bird-or-egg) is a metaphor describing situations where it is not clear which of two interrelated events or processes is the cause and which the effect. Plutarch was the first to pose this type of causality as a philosophical problem using the example of the hen and the egg, as indicated in the motto above.[*]

The objective of the paper is to demonstrate that relations of atmospheric $CO_2$ and temperature may qualify into the category of "hen-or-egg" problems, where it is not always clear which of two interrelated events is the cause and which the effect. First, we discuss the relationships between temperature and $CO_2$ concentration and specifically intriguing results from proxy data-based palaeoclimatic study, where change in temperature leads and change in $CO_2$ concentration follows. Next, we discuss the data bases of modern (instrumental) measurements, related to global temperature and atmospheric $CO_2$ concentration and introduce a methodology to analyse them. We develop a stochastic framework, introducing useful notions of time irreversibility and system causality. In the results section, we examine the relationship of global temperature and carbon dioxide concentration using the modern data, available at the monthly time step. We juxtapose time series of global temperature and atmospheric $CO_2$ concentration from several sources, covering the common time interval 1980-2019. In our methodology, it is the timing, rather than the magnitude, of changes that is important, being the determinant of causality. When examining time series of global records, we found situations when change in temperature leads and change in $CO_2$ concentration follows. Interpretation of cross-correlation of time series of global temperature and atmospheric $CO_2$ supports the "hen-or-egg" hypothesis, indicating that both causality directions exist, while ($T \rightarrow CO_2$) dominates. We attempt to interpret this mechanism by noting the positive feedback loop—higher temperatures increase soil respiration and, hence, $CO_2$ emission.

The analysis reported in this paper was prompted by observation of an unexpected (and unfortunate) real-world experiment: during the Covid-19 lockdown in 2020, despite unprecedented decrease in carbon emissions demonstrated in various sources (example given in Figure 1), there was increase in atmospheric $CO_2$ concentration, which followed a pattern similar to previous years (Figure 2). Indeed, global $CO_2$ emissions were over 5% lower in the first quarter of 2020 than in that of 2019, mainly due to an 8% decline in emissions from coal, 4.5% from oil and 2.3% from natural gas (IEA, 2020). However, the normal pattern of atmospheric $CO_2$ concentration (increase until May and decrease in June) did not change. Similar was the behaviour after the 2008-09 financial crisis, but the most recent situation is more characteristic because the Covid-19 decline in 2020 is the severest ever, even from those in the

[*] We note that in the original Greek text "ἡ ὄρνις" is feminine (article and noun) meaning the hen, rather than the chicken. Therefore, here we preferred the form "hen-or-egg" over "chicken-or-egg", which is more common in English. Very often, in online Greek texts (e.g. https://el.wikisource.org/wiki/Συμποσιακά_Β΄), "ἡ ὄρνις" appears as "ἡ ἄρνις" (again feminine but with an 'α' rather than 'ο'; this form was also reproduced in Koutsoyiannis, 2019). After extended search, we contend that this must be an error, either an old one in manuscript copying (e.g. by monks in monasteries) or a modern one (in OCR, as we met the same error in several other Greek texts). We are confident that the correct word is "ὄρνις".

World Wars. It is also noteworthy in Figure 1 that there were three years in sequel without major increase in 2010s,[*] where again there was increase in $CO_2$ concentration.

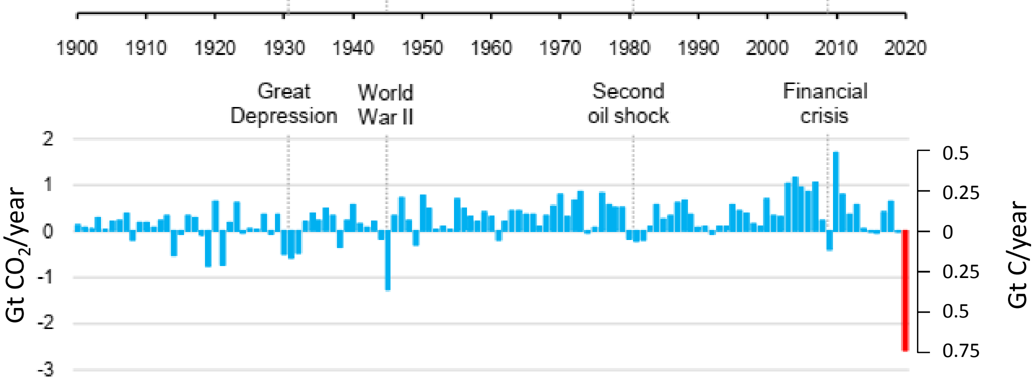


**Figure 1.** Annual change in global energy-related $CO_2$ emissions (adapted from IEA, 2020)

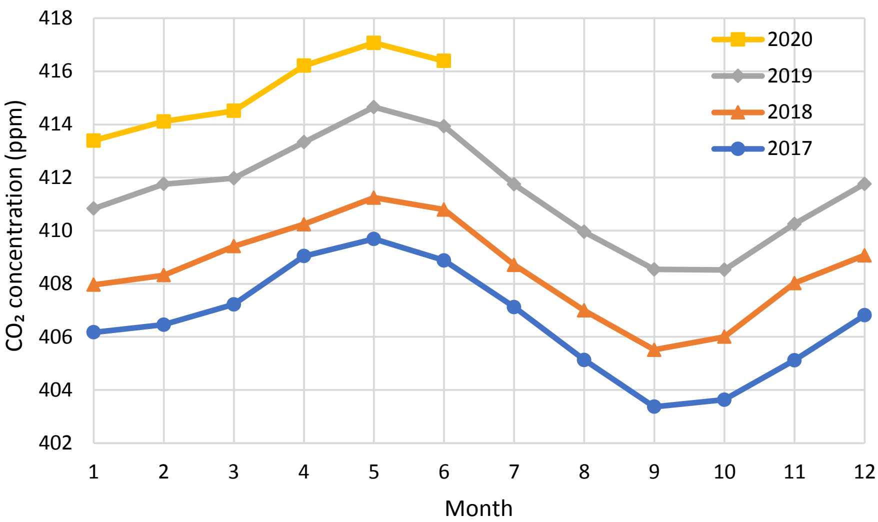


**Figure 2.** Atmospheric $CO_2$ concentration measured in Mauna Loa, Hawaii, USA, in the last four years.

# 2 Temperature and carbon dioxide – From Arrhenius to palaeo-proxies

Does the relationship of atmospheric carbon dioxide ($CO_2$) and temperature classify as a "hen-or-egg" type causality? If we look at the first steps of studying the link between the two, the reply is clearly negative. Arrhenius (1896), the first scientist who proposed the causal relationship between atmospheric carbon dioxide concentration and temperature, regarded the changes of the latter as the cause and the changes of the former as the effect. Specifically, he stated:

> *Conversations with my friend and colleague Professor Högbom together with the discussions above referred to, led me to make a preliminary estimate of the probable effect of a variation of the atmospheric carbonic acid* [meant $CO_2$] *on the temperature of the earth. As this estimation led to the belief that one might in this way probably find an explanation for*

[*] At first glance, this does not sound reasonable and therefore we have cross-checked the data with another source (Global Carbon Atlas, http://www.globalcarbonatlas.org/en/CO2-emissions; see also Our World In Data, https://ourworldindata.org/grapher/annual-co-emissions-by-region) and we found only slight differences. Interestingly, **Error! Reference source not found.** also shows a rapid growth in emissions after the 2008–09 global financial crisis, which agrees with Peters et al. (2012).

*temperature variations of 5°-10° C, I worked out the calculation more in detail and lay it now before the public and the critics.*

Furthermore, following the Italian meteorologist De Marchi (1895), whom he cited, he rejected what we call today *Milanković cycles* as possible causes of the glacial periods. In addition, he substantially overestimated the role of $CO_2$ in the greenhouse effect of the Earth's atmosphere. He calculated the relative weights of absorption of $CO_2$ and water vapour as 1.5 and 0.88, respectively, a ratio of 1:0.6.

Arrhenius (1896) also stated that "*if the quantity of carbonic acid increases in geometric progression, the augmentation of the temperature will increase nearly in arithmetic progression*". This Arrhenius's "rule" (which is still in use today) is mathematically expressed as:

$$T - T_0 = \alpha \ln\left(\frac{[CO_2]}{[CO_2]_0}\right) \quad (1)$$

where $T$ and $[CO_2]$ denote temperature and $CO_2$ concentration, respectively, $T_0$ and $[CO_2]_0$ represent reference states, and $\alpha$ is a constant.

However, while the fact that the two variables are tightly connected is beyond doubt, the direction of the simple causal relationship needs to be studied further.

Today additional knowledge has been accumulated, particularly from palaeoclimatic studies, which allow us to examine Arrhenius's hypotheses on a sounder basis. In brief, we can state the following:

- Indeed, $CO_2$ plays a substantial role as a greenhouse gas. However, modern estimates of the $CO_2$ contribution to the greenhouse effect largely differ from Arrhenius's results, attributing 19% of the long-wave radiation absorption to $CO_2$ against 75% of water vapour and clouds (Schmidt et al., 2010), a ratio of 1:4.
- During the Phanerozoic Eon, Earth's temperature has varied by even more than 5-10 °C, which was postulated by Arrhenius (see Figure 3). The link of temperature and $CO_2$ is beyond doubt, even though it is not clear in Figure 3. It becomes more legible in proxy data of the Quaternary (see Figure 4). As seen in Figure 3, the $CO_2$ concentration has varied by about two orders of magnitude.
- It has been demonstrated in a persuasive manner (Roe, 2006) that in the Quaternary it is the effect of Milanković cycles (variations in eccentricity, axial tilt, and precession of Earth's orbit), rather than of atmospheric $CO_2$ concentration, that explains the glaciation process. Specifically (quoting Roe, 2006):

  *variations in atmospheric $CO_2$ appear to lag the rate of change of global ice volume. This implies only a secondary role for $CO_2$ —variations in which produce a weaker radiative forcing than the orbitally-induced changes in summertime insolation— in driving changes in global ice volume.*

Despite falsification of some of Arrhenius's hypotheses, his line of thought remained dominant.

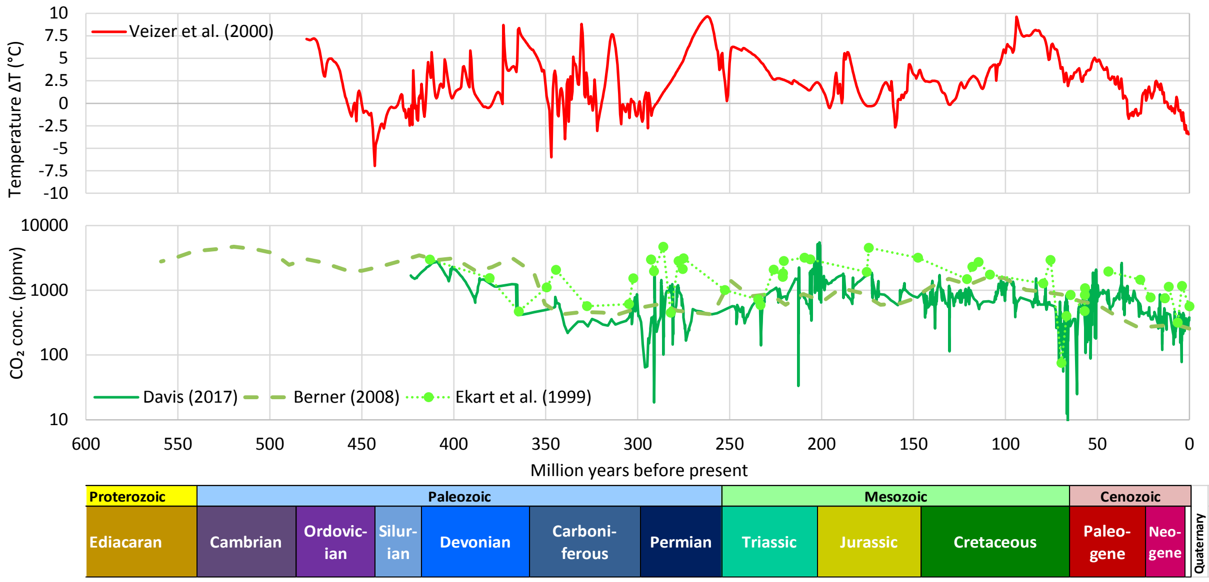


**Figure 3.** Proxy-based reconstructions of temperature, and $CO_2$ concentration during the Phanerozoic Eon. The original figures by Veizer et al. (2000), Davis (2017), Berner (2008) and Ekart et al. (1999) were digitized in this study. The chronologies of geologic eras shown in the bottom of the figure have been taken from the International Commission on Stratigraphy (https://stratigraphy.org/chart).

Yet there have been some important studies, based on palaeoclimatological reconstructions (mostly the Vostok ice cores, Jouzel et al., 1987; Petit et al. 1999), which have pointed to the opposite direction of causality, i.e. the change of temperature as the cause and that in the $CO_2$ concentration as the effect. Such claims have explained the fact that temperature change leads and $CO_2$ concentration change follows. In agreement with Roe (2006), several papers have found the time lag positive, with estimates varying from 50 to 1000 years, depending on the time period and the particular study (Caillon et al., 2003; Soon, 2007; Pedro et al., 2012; Koutsoyiannis, 2019; Chowdhry Beeman et al., 2019). Claims that $CO_2$ concentration leads (i.e., a negative lag) have not been generally made by these authors. At most a synchrony claim has been sought, on the basis that the estimated positive lags are often within the 95% uncertainty range (Chowdhry Beeman et al., 2019), while Pedro et al. (2012) has asserted that a "short lead of $CO_2$ over temperature cannot be excluded".

Surprisingly however, to our knowledge, there have been no studies of this type (i.e. by exploring the wealth of existing data rather than fitting models), about the causal relation between temperature and $CO_2$, based on the rich body of modern datasets.

Since palaeoclimatic data suggest a direction opposite to that assumed by Arrhenius, Koutsoyiannis (2019), using palaeoclimatic data from the Vostok ice cores at a time resolution of 1000 years and a stochastic framework similar to that of the present study (see section 3.2) concluded that change in temperature precedes that of $CO_2$ by one time step (1000 years), as illustrated in Figure 7. He also noted that this "*causality condition holds for a wide range of time lags, up to 26 000 years, and hence the time lag is positive and most likely real.*" He asserted that the problem is obviously more complex than that of exclusive roles of cause and effect, classifying it in the hen-or-egg causality problems. Obviously, however, the proxy character of these data and the too large time step of the time series reduce the reliability and accuracy of the results.

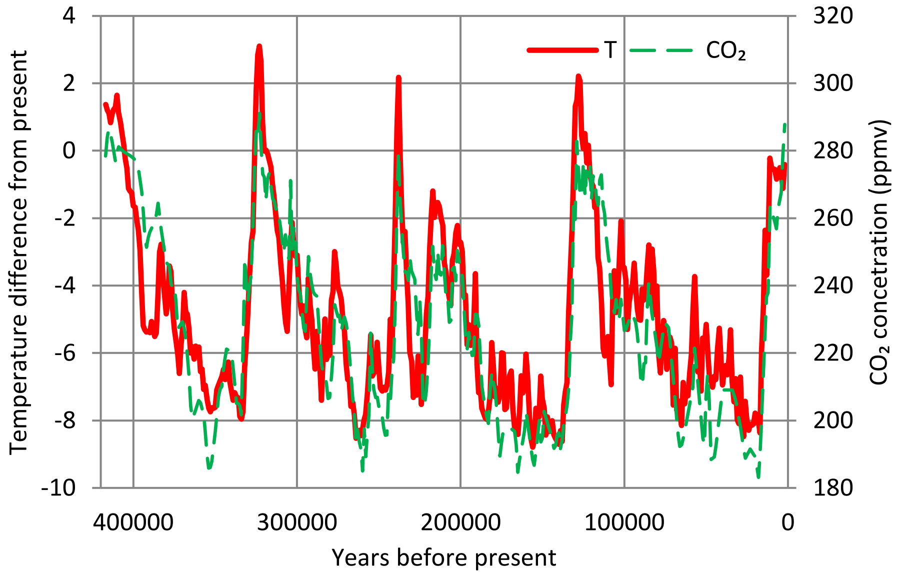


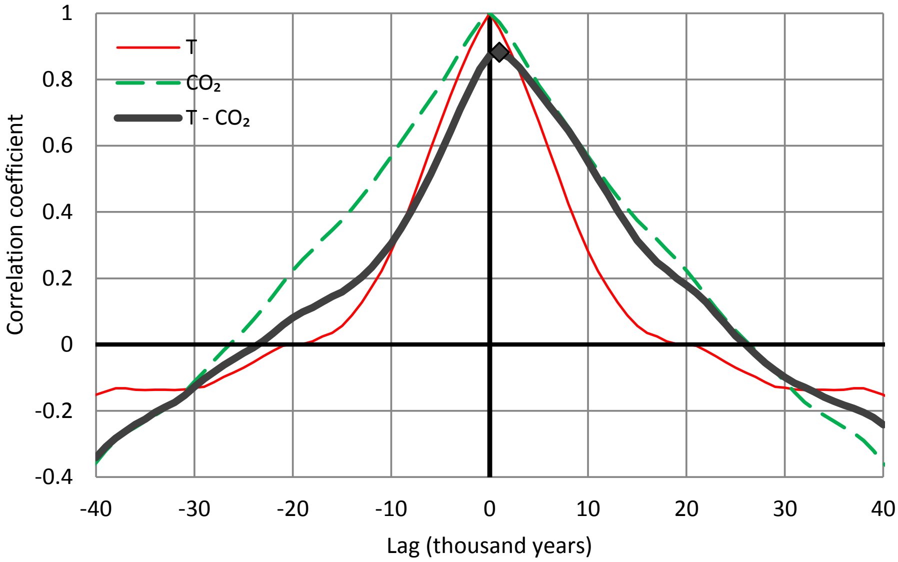


**Figure 4.** (Upper) Time series of temperature and $CO_2$ concentration from the Vostok ice core, covering part of the Quaternary (420 000 years) with time step of 1000 years. (Lower) Auto- and cross-correlograms of the two time series. The maximum value of the cross-correlation coefficient is 0.88 and appears at lag 1 thousand years (Adapted from Koutsoyiannis, 2019).

# 3 Data and methods

## 3.1 Data sets

Our investigation of the relationship of temperature and concentration of carbon dioxide in the atmosphere is based on two time series of the former process and four of the latter. Specifically, the temperature data are of two origins, satellite and ground based. The satellite dataset, developed at the University of Alabama in Huntsville (UAH), infers the temperature, *T*, of three broad levels of the atmosphere from satellite measurements of the oxygen radiance in the microwave band, using advanced (passive) microwave sounding units on NOAA and NASA satellites (Spencer and Christy, 1990; Christy et al., 2007). The data are publicly available on monthly scale in the forms of time series of “anomalies” (defined as differences from long-term means) for several parts of earth, as well as in maps. Here we use only the global average on monthly scale for the lowest level, referred to as the lower troposphere. The ground-based data series we used is the CRUTEM.4.6.0.0 global T2m land temperature (Jones et al., 2012). This originates from a gridded dataset of historical near-surface air temperature anomalies over land. Data are available for each month from January 1850 to present. The dataset is a collaborative product of the Met Office Hadley Centre and the Climatic Research Unit at the University of East Anglia.

The two temperature series used in the study are depicted in Figure 5. They are consistent to each other (and correlated, $r = 0.8$), yet the CRUTEM4 series shows a larger increasing trend than the UAH series. The differences are explainable by three reasons: (a) the satellite series includes both land and sea, while the ground based is for land only, in which the increasing trend is substantially higher than in sea; the satellite series refers to some high altitude in the troposphere (see Koutsoyiannis, 2020), while the ground-based series refers to the ground level; and (c) the ground-based series is affected by urbanization (a lot of ground stations are located in urban areas). In any case, the difference in the increasing trends is irrelevant for the current study, as the timing, rather than the magnitude, of changes is the determinant of causality.

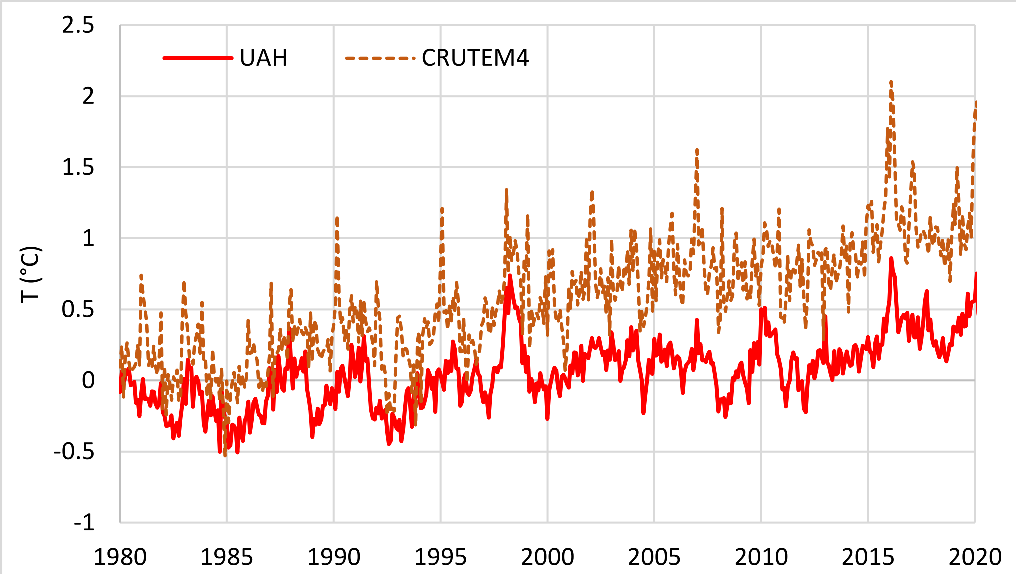


**Figure 5.** Plots of the data series of global temperature anomalies since 1980, as used in the study, from satellite measurements over the globe (UAH) and from ground measurements over land (CRUTEM4).

The most famous $CO_2$ data set is that of Mauna Loa Observatory (Keeling et al., 1976). The Observatory, located on the north flank of Mauna Loa Volcano, on the Big Island of Hawaii, USA, at an elevation of 3397 m above sea level, is a premier atmospheric research facility that has been continuously monitoring and collecting data related to the atmosphere since the 1950s. The NOAA has also other stations that systematically measure atmospheric $CO_2$ concentration, namely at Barrow, Alaska, USA and at South Pole. The NOAA's Global Monitoring Laboratory Carbon Cycle Group also computes global mean surface values of $CO_2$ concentration using measurements of weekly air samples from the Cooperative Global Air Sampling Network. The global estimate is based on measurements from a subset of network sites. Only sites where samples are predominantly of well-mixed marine boundary layer air, representative of a large volume of the atmosphere, are considered (typically at remote marine sea level locations with prevailing onshore winds). Measurements from sites at high altitude (such as Mauna Loa) and from sites close to anthropogenic and natural sources and sinks are excluded from the global estimate.[*]

The period of data coverage varies, but all series cover the common 40-year period 1980-2019, which hence constituted the time reference of all our analyses. As a slight exception, the Barrow (Alaska) and South Pole measurements have not yet been available in final form for 2019 and, thus, this year was not included in our analyses of these two time series. The data of the latter two stations are given in irregular-step time series, which was regularized to monthly in this study. All other data series have already been available on monthly scale.

All four $CO_2$ time series used in the study are depicted in Figure 6. They show a superposition of increasing trends and annual cycles whose amplitudes increase as we head from the South to the North Pole. The South Pole series has opposite phase of oscillation compared to the other three. The annual cycle is better seen in Figure 7, where we have removed the trend with standardization, namely by dividing each monthly value by the geometric average of the 5-year period before it. The reason why we used division rather than subtraction and geometric rather than arithmetic average (being thus equivalent to subtracting or averaging the logarithms of $CO_2$ concentration), will become evident in section 4. In the right panel of Figure 7, which depicts monthly statistics of the time series of the left panel, it is seen that in all sites but the South Pole the annual maximum occurs in May; that of the South Pole occurs in September.

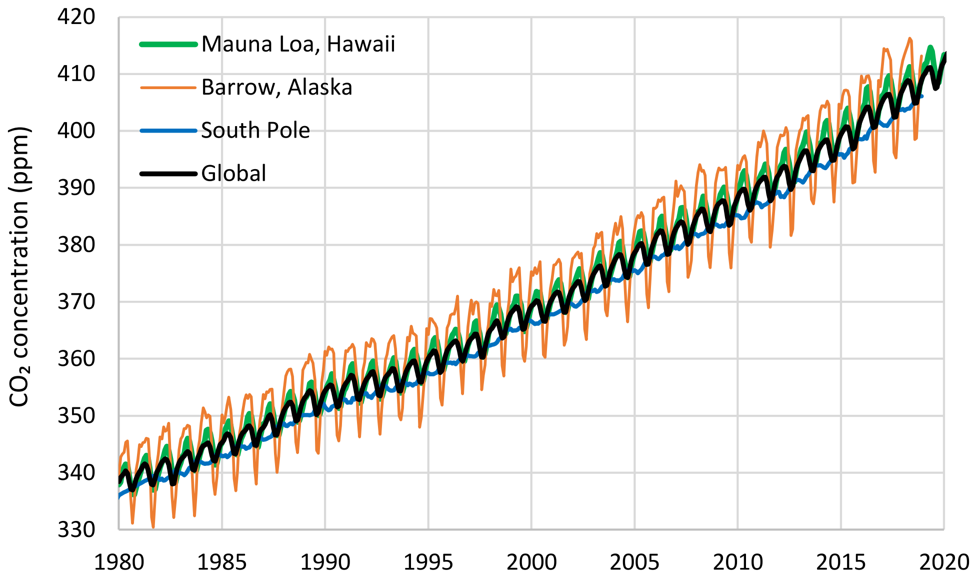


**Figure 6.** Plots of the data series of atmospheric $CO_2$ concentration measured in Mauna Loa (Hawaii, USA), Barrow (Alaska, USA) and South Pole, and global average.

* Details about this data set are provided in https://www.esrl.noaa.gov/gmd/ccgg/about/global_means.html.

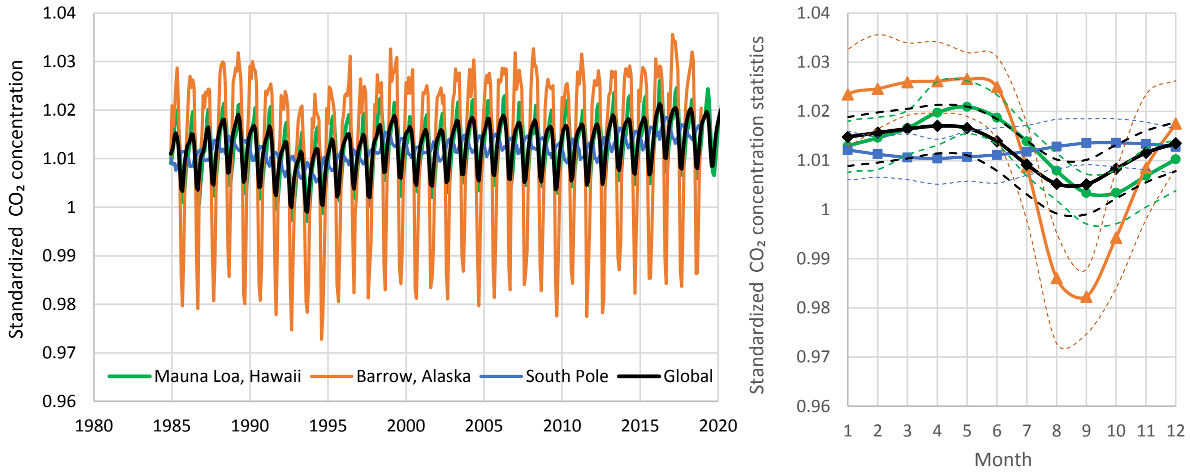


**Figure 7.** Plots of atmospheric $CO_2$ concentration after standardization: (Left) Each monthly value is standardized by dividing with the geometric average of the 5-year period before it. (Right) Monthly statistics of the values of the left panel; for each month the average is shown in continuous line and the minimum and maximum in thin dashed lines of the same colour as the average.

## 3.2 Stochastic framework

A recent study (Koutsoyiannis, 2019) has investigated time irreversibility in hydrometeorological processes and developed a theoretical framework in stochastic terms. It also studied necessary conditions for causality, which is tightly tied to time irreversibility. A simple definition of time reversibility within stochastics is the following, where underlined symbols denote stochastic (random) variables and non-underlined ones denote values thereof or regular variables.

A stochastic process $\underline{x}(t)$ at continuous time $t$, with $n$th order distribution function:

$$F(x_1, x_2, \dots, x_n; t_1, t_2, \dots, t_n) := P\{\underline{x}(t_1) \le x_1, \underline{x}(t_2) \le x_2, \dots, \underline{x}(t_n) \le x_n\} \tag{2}$$

is time-symmetric or time-reversible if its joint distribution does not change after reflection of time about the origin, i.e., if for any $n, t_1, t_2, \dots, t_n$,

$$F(x_1, x_2, \dots, x_n; t_1, t_2, \dots, t_n) = F(x_1, x_2, \dots, x_n; -t_1, -t_2, \dots, -t_n) \tag{3}$$

If times $t_i$ are equidistant, i.e. $t_i - t_{i-1} = D$, the definition can be also written by reflecting the order of points in time, i.e.:

$$F(x_1, x_2, \dots, x_{n-1}, x_n; t_1, t_2, \dots, t_{n-1}, t_n) = F(x_1, x_2, \dots, x_{n-1}, x_n; t_n, t_{n-1}, \dots, t_2, t_1) \tag{4}$$

A process that is not time-reversible is called time-asymmetric, time-irreversible or time-directional. Important results related to time (ir)reversibility are the following:

- A time reversible process is also stationary (Lawrance, 1991).
- If a scalar process $\underline{x}(t)$ is Gaussian (i.e., all its finite dimensional distributions are multivariate normal) then it is reversible (Weiss, 1975). The consequences are: (a) a directional process cannot be Gaussian; (b) a discrete-time ARMA process (and a continuous-time Markov process) is reversible if and only if it is Gaussian.
- However, a vector (multivariate) process can be Gaussian and irreversible at the same time. A multivariate Gaussian linear process is reversible if and only if its autocovariance matrices are all symmetric (Tong and Zhang, 2005).

Time asymmetry of a process can be studied more conveniently (or even exclusively in a scalar process) through the differenced process, i.e.:

$$\underline{\tilde{x}}_{\tau,\nu} \coloneqq \underline{x}_{\tau+\nu} - \underline{x}_{\tau} \tag{5}$$

for an appropriate time-step $\nu$ of differencing. The differenced process represents change of the original process within a time period of length $\nu$. We further define the cumulative process of $\underline{x}_{\tau}$ for discrete time $\kappa$ as:

$$\underline{X}_{\kappa} \coloneqq \underline{x}_1 + \underline{x}_2 + \cdots + \underline{x}_{\kappa} \tag{6}$$

The time average of the original process $\underline{x}_{\tau}$ for discrete time scale $\kappa$ is

$$\underline{x}_{\tau}^{(\kappa)} \coloneqq \frac{\underline{x}_{(\tau-1)\kappa+1} + \underline{x}_{(\tau-1)\kappa+2} + \cdots + \underline{x}_{\tau\kappa}}{\kappa} = \frac{\underline{X}_{\tau\kappa} - \underline{\tilde{X}}_{(\tau-1)\kappa}}{\kappa} \tag{7}$$

Similar equations for the cumulative and averaged processes for the differenced process $\underline{\tilde{x}}_{\tau,\nu}$ are given in Appendix A.

The variance of the process $\underline{x}_{\tau}^{(\kappa)}$ is a function of the time scale $\kappa$ which is termed the climacogram of the process:

$$\gamma_{\kappa} \coloneqq \operatorname{var}\left[\underline{x}_{\tau}^{(\kappa)}\right] \tag{8}$$

The autocovariance function for time lag $\eta$ is derived from the climacogram through the relationship (Koutsoyiannis, 2016):

$$c_{\eta} = \frac{(\eta+1)^2\gamma_{|\eta+1|} + (\eta-1)^2\gamma_{|\eta-1|}}{2} - \eta^2\gamma_{|j|} \tag{9}$$

For sufficiently large $\kappa$ (theoretically as $\kappa \to \infty$), we may approximate the climacogram as:

$$\gamma_{\kappa} \propto \kappa^{2H-2} \tag{10}$$

where $H$ is termed the *Hurst parameter*. The theoretical validity of such (power-type) behaviour of a process was implied by Kolmogorov (1940). The quantity $2H-2$ is visualized as the slope of the double logarithmic plot of the climacogram for large time scales. In a random process, $H = 1/2$, while in most natural processes $1/2 \leq H \leq 1$, as first observed by Hurst (1951). This natural behaviour is known as (long-term) *persistence* or *Hurst-Komogorov* (HK) *dynamics*. A high value of $H$ (approaching 1) indicates enhanced presence of patterns, enhanced change and enhanced uncertainty (e.g. in future predictions). A low value of $H$ (approaching 0) indicates enhanced fluctuation or *antipersistence* (sometimes misnamed as quasi-periodicity, as the period is not constant).

For a stationary stochastic process $\underline{x}_{\tau}$, the differenced process $\underline{\tilde{x}}_{\tau}$ has mean zero and variance:

$$\tilde{\gamma}_{\nu,1} \coloneqq \operatorname{var}\left[\underline{\tilde{x}}_{\tau,\nu}\right] = \operatorname{var}\left[\underline{x}_{\kappa+\nu}\right] + \operatorname{var}\left[\underline{x}_{\tau}\right] - 2\operatorname{cov}\left[\underline{x}_{\tau+\nu}, \underline{x}_{\tau}\right] = 2(\gamma_1 - c_{\nu}) \tag{11}$$

where $\gamma_1$ and $c_{\nu}$ are the variance and lag $\nu$ autocovariance, respectively, of $\underline{x}_{\tau}$. Furthermore, as demonstrated by Koutsoyiannis (2019), the Hurst coefficient of the differenced process $\underline{\tilde{x}}_{\tau}$ precisely equals zero, which means that $\underline{\tilde{x}}_{\tau}$ is completely antipersistent, irrespective of $\gamma_{\kappa}$.

As the first moment (mean) of the differenced process is always zero (provided that the original process is stationary), while the second one (variance) is always positive and thus it does not provide indications on time asymmetry, in a scalar process the least-order moment that can be used to detect reversibility is the third, $\mu_3\left[\underline{\tilde{x}}_{\tau,\nu}\right]$, or equivalently, the skewness coefficient:

$$\tilde{C}_{S_\nu} \coloneqq \frac{\mu_3\left[\underline{\tilde{x}}_{\tau,\nu}\right]}{\left(\operatorname{var}\left[\underline{\tilde{x}}_{\tau,\nu}\right]\right)^{3/2}} \tag{12}$$

Processes with large $\tilde{C}_{S_\nu}$ signify high (positive) time irreversibility. Gaussian processes, in which the skewness is zero, are necessarily time symmetric, as already mentioned.

However, in vector processes, to study irreversibility we can use second order moments, and in particular cross-covariances among the different components of the vector. In particular (simplifying the analyses and results in Koutsoyiannis, 2019), given two processes $\underline{x}_\tau$ and $\underline{y}_\tau$ we could study the cross-correlations:

$$r_{\tilde{x}\tilde{y}}[\nu,\eta] = \operatorname{corr}\left[\underline{\tilde{x}}_{\tau,\nu}, \underline{\tilde{y}}_{\tau+\eta,\nu}\right] \tag{13}$$

Time (ir)reversibility could then be characterized by studying the properties of symmetry or asymmetry of $r_{\tilde{x}\tilde{y}}(\nu,\eta)$ as a function of the time lag $\eta$. In a symmetric bivariate process, $r_{\tilde{x}\tilde{y}}[\nu,\eta]$ = $r_{\tilde{x}\tilde{y}}[\nu,-\eta]$ and if the two components are positively correlated, the maximum of $r_{\tilde{x}\tilde{y}}[\nu,\eta]$ will appear at lag $\eta = 0$. If the bivariate process is irreversible, this maximum will appear at a lag $\eta_1 \neq 0$ and its value will be $r_{\tilde{x}\tilde{y}}[\nu,\eta_1]$.

Time asymmetry is closely related to causality, which presupposes irreversibility. Thus, "*no causal process (i.e., such that of two consecutive phases, one is always the cause of the other) can be reversible*" (Heller 1983; see also Kline 1980). In probabilistic definitions of causality, time asymmetry is determinant. Thus, Suppes (1970) defines causation as "*An event $B_{t'}$* [occurring at time $t'$] *is a prima facie cause of the event $A_t$ if and only if (i) $t' < t$, (ii) $P\{B_{t'}\} > 0$, (iii) $P(A_t|B_{t'}) > P(A_t)$.*" Also, Granger's (1980) first axiom in defining causality reads "*The past and present may cause the future, but the future cannot.*"

Consequently, in simple causal systems, in which the process component $\underline{x}_\tau$ is the cause of $\underline{y}_\tau$ (like in the case of rainfall ($\underline{x}_\tau$) and runoff ($\underline{y}_\tau$)), it is reasonable to expect $r_{\tilde{x}\tilde{y}}[\nu,\eta] \geq 0$ for any $\eta \geq 0$, while $r_{\tilde{x}\tilde{y}}[\nu,\eta] = 0$ for any $\eta = 0$. However, in hen-and-egg causal systems, this will not be the case and we reasonably expect $r_{\tilde{x}\tilde{y}}[\nu,\eta] \neq 0$ for any $\eta$. Yet, we can define a dominant direction of causality based on the cross-correlation maximizing time lag $\eta_1$, formally defined for a specified $\nu$ as:

$$\eta_1 \coloneqq \arg\max |r_{\tilde{x}\tilde{y}}(\nu,\eta)| \tag{14}$$

We can thus distinguish the following three cases:

- If $\eta_1 = 0$ then there is no dominant direction.
- If $\eta_1 > 0$ then the dominant cause is $\underline{x}_\tau$.
- If $\eta_1 < 0$ then the dominant cause is $\underline{y}_\tau$.

Further explanations are provided in Appendix B. It must be stressed that the above conditions are put as necessary and not sufficient conditions for a causative relationship between the processes $\underline{x}_\tau$ and $\underline{y}_\tau$. Following Koutsoyiannis (2019), we avoid seeking sufficient conditions, a task that would be too difficult or impossible due to its deep philosophical complications. Additional necessary conditions can be found in Koutsoyiannis (2019).

# 4 Results

Here we examine the relationship of atmospheric temperature and carbon dioxide concentration using the modern data (observations rather than proxy), available at the monthly time step, as described in section 3. To apply our stochastic framework, we must first make the two time series linearly compatible. Specifically, based on Arrhenius's rule (equation (1)), we take the logarithms of $CO_2$ concentration, while we keep $T$ untransformed. We then construct the differenced processes, which quantify changes. Taking differences is physically meaningful as both $CO_2$ concentration and temperature (equivalent to thermal energy) represent "stocks", i.e. stored quantities, and, thus, indeed the mass and energy fluxes are represented by differences.

The time step of differencing was chosen equal to one year ($\nu$ = 12 for the monthly time step of the time series). For instance, from the value of January of a certain year we subtract the value of January of the previous year and so forth. A first reason for this choice is that it almost eliminates the effect of the annual cycle (periodicity). A second reason is that the temperature data are given in terms of "anomalies", i.e., differences from an average which varies from month to month. By taking $\nu = 12$, the varying means are eliminated and "anomalies" are effectively replaced by the actual processes (as the differences in the actual values equal the differences of "anomalies").

We perform all analyses on monthly and annual time scales. Figure 8 shows the differenced time series for the UAH temperature and Mauna Loa $CO_2$ concentration at monthly scale; the symbols $\Delta T$ and $\Delta \ln[CO_2]$ are used interchangeably with $\underline{\tilde{x}}_{\tau,12}$ and $\underline{\tilde{y}}_{\tau,12}$, respectively. It may be observed that most often the temperature curve leads and that of $CO_2$ follows. However, there are cases where the changes in the two processes synchronize in time or even become decoupled.

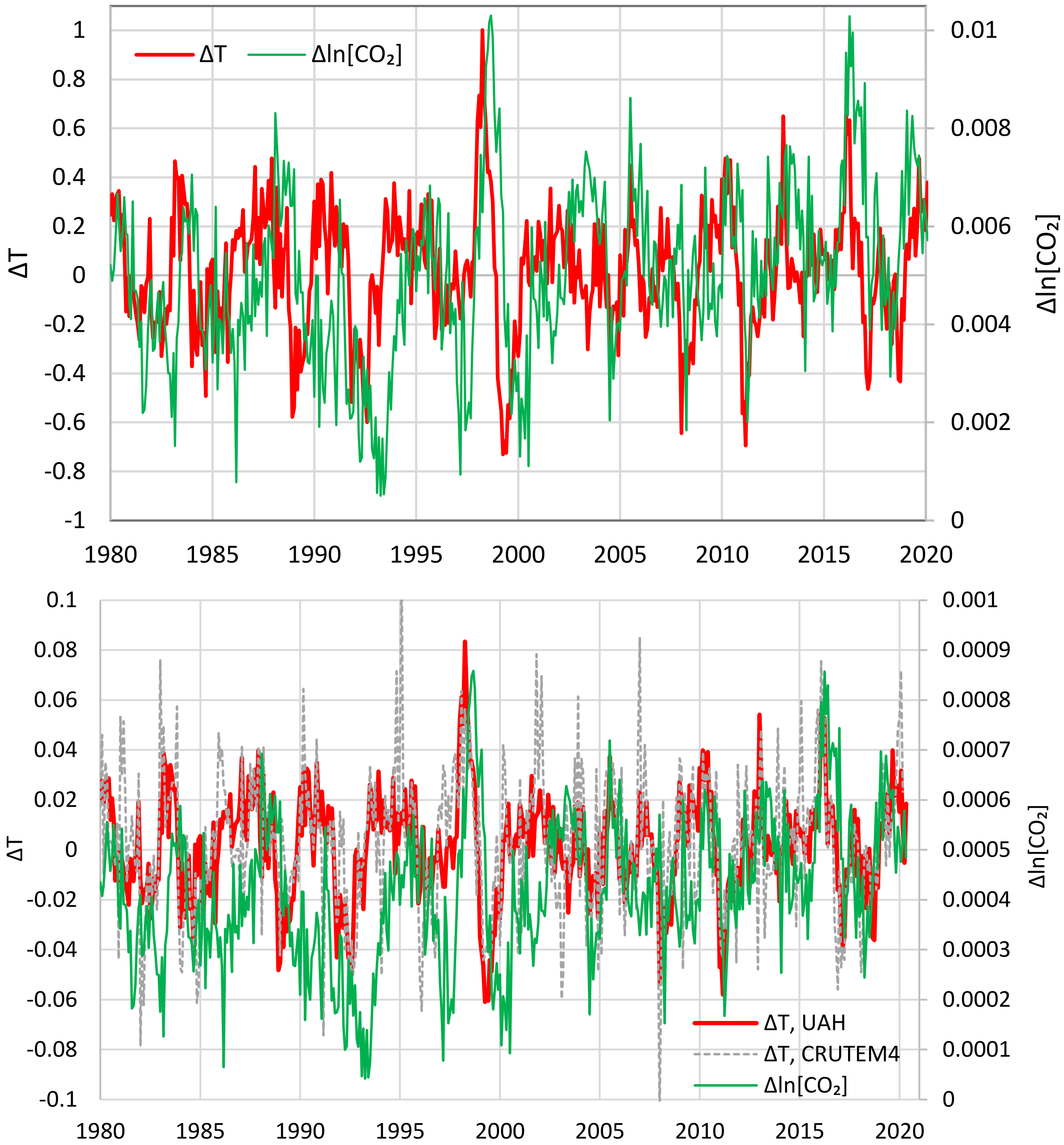


Figure 8. Differenced time series of UAH temperature and logarithms of $CO_2$ concentrations at Mauna Loa at monthly scale. The graph in the upper panel was constructed in the manner described in the text. The graph in the lower panel is given for comparison and was constructed differently, by taking differences of the values of each month with the previous month and then averaging over the previous 12 months (to remove periodicity); in addition, the lower graph includes the CRUTEM4 land temperature series.

Figure 9 shows the same time series at the annual time scale, with the year being defined as July-June for $\Delta T$ and February-January for $\Delta \ln[CO_2]$. The reason for this differentiation will be explained in the next section. Here it is more evident that most of the time the temperature change leads and that of $CO_2$ follows.

It is of interest here that the variability of global mean annual temperature is significantly influenced by the rhythm of ocean-atmosphere oscillations, such as ENSO, AMO and IPO (Kundzewicz et al., 2020). This mechanism may be a complicating factor, in turn influencing the link between temperature and $CO_2$ concentration.

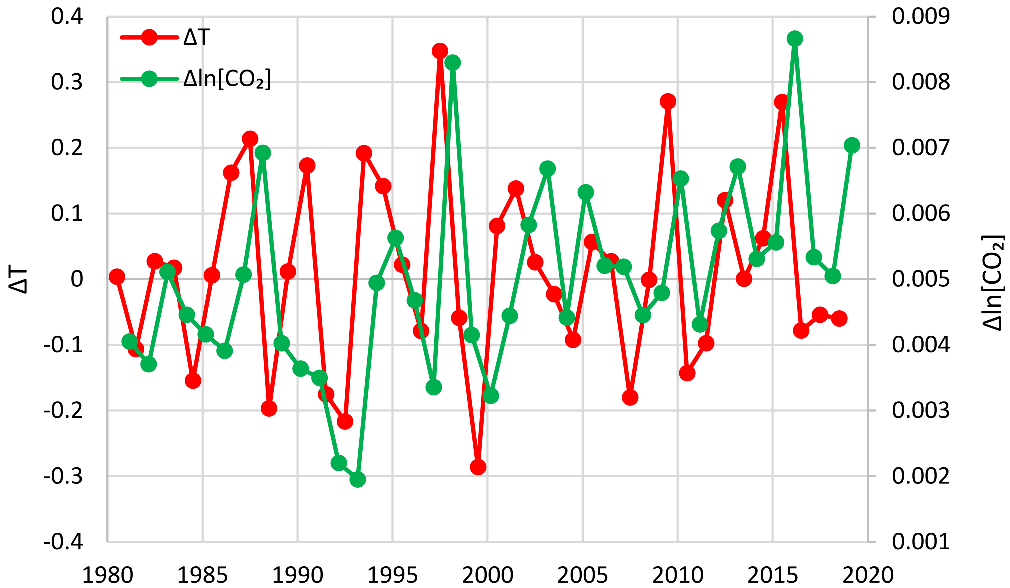


Figure 9. Annually averaged time series of differenced temperatures (UAH) and logarithms of $CO_2$ concentrations (Mauna Loa). Each dot represents the average of a one-year duration ending at the time of its abscissa.

The climacograms of the differenced time series used (actually four of the six to avoid an overcrowded graph) are shown in Figure 10. It appears that the differenced temperature time series are consistent with the condition implied by stationarity, i.e., $H$ = 0 for the differenced process. The same does not look to be the case for the $CO_2$ time series, particularly for the Mauna Loa time series, in which the Hurst parameter appears to be close to 1/2. Based on this, one would exclude stationarity for the Mauna Loa $CO_2$ time series. However, a simpler interpretation of the graph is that the data record is not long enough to reveal that $H$ = 0 for the differenced process. Actually, all available data belong to a period in which [$CO_2$] exhibits a monotonic increasing trend (as also verified by the fact that all values of $\Delta \ln[CO_2]$ in Figure 8 and Figure 9 are positive, while stationarity entails a zero mean of the differenced process). Had the available data base been broader, both positive and negative trends could appear. Indeed, a broader view of the [$CO_2$] process, based on palaeoclimatic data (Figure 4) would justify a stationarity assumption.

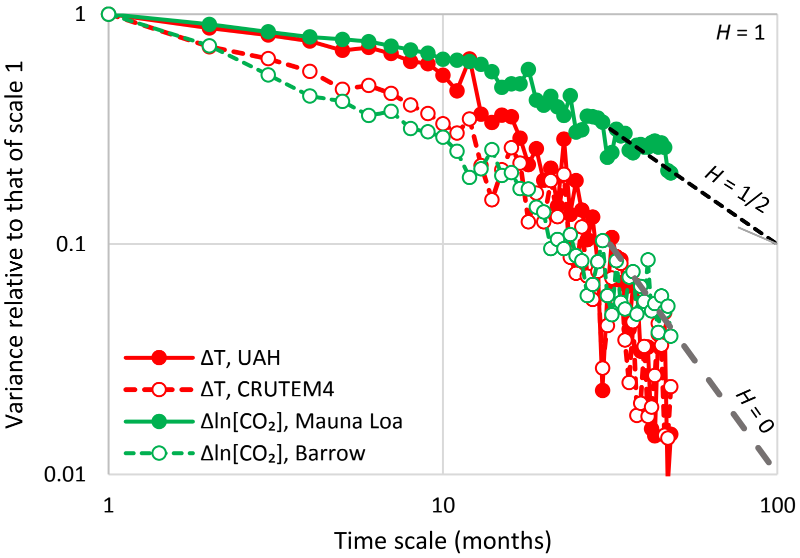


Figure 10. Empirical climacograms of the indicated differenced time series; the characteristic slopes corresponding to values of the Hurst parameter $H$ = 1/2 (large-scale randomness), 0 (full antipersistence) and 1 (full persistence) are also plotted (note, $H$ = 1 – slope/2),

A preliminary qualitative observation from graphical inspection of Figure 8 and Figure 9, suggests that the temperature change very often precedes and the $CO_2$ change follows—in the same direction. We note, though, that temperature changes alternate in sign while $CO_2$ changes are always positive.

A quantitative analysis, based on the methodology in section 3.2, requires the study of lagged cross-correlations of the two processes. Figure 11 shows the cross-correlogram between UAH temperature and Mauna Loa $CO_2$ concentration; the autocorrelograms of the two processes are also plotted for comparison. The fact that the cross-correlogram does not have values consistently close to zero at any of the semi-axes eliminates the possibility of an exclusive (unidirectional) causality and suggests consistency with "hen-or-egg" causality.

The maximum cross correlation of the monthly series is 0.47 and appears at a positive lag, $\eta_1$ = 5 months, thus suggesting temperature, rather than $CO_2$, as dominant cause. Similar are the graphs of the other combinations of temperature and $CO_2$ data sets, which are shown in Appendix C. In all cases $\eta_1$ is positive, ranging from 5 to 11 months.

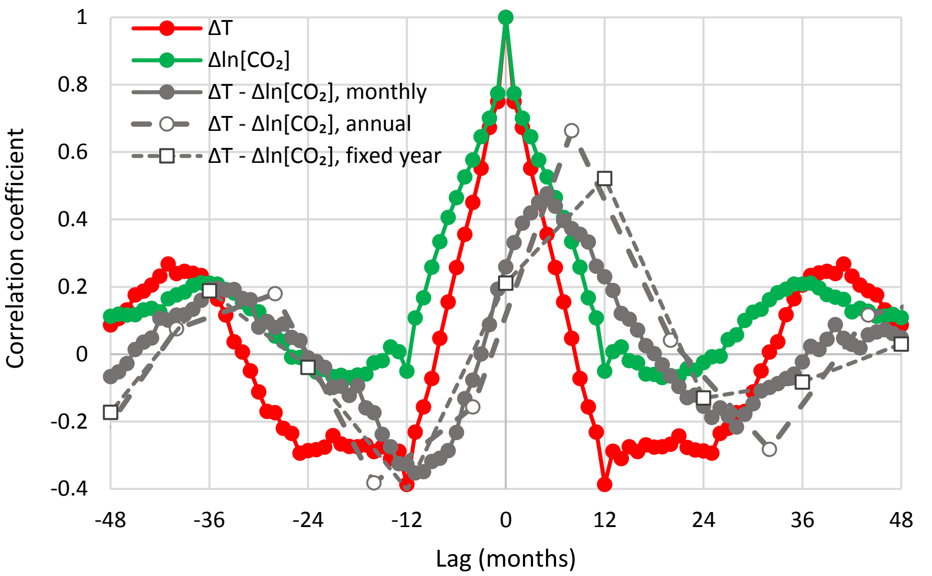

Figure 11. Auto- and cross-correlograms of the differenced time series of UAH temperature and Mauna Loa $CO_2$ concentration.

To perform similar analyses on the annual scale, we fixed the specification of a year for temperature for the period July-June, as already mentioned, and then slid the initial month specifying the beginning of a year for $CO_2$ concentration so as to find a specification that maximizes the cross-correlation at the annual scale. In Figure 11, maximization occurs when the year specification is February-January (of the next year), i.e., if the lag is 8 months. The maximum cross-correlation is 0.66. If we keep the specification of the year for $CO_2$ concentration same as in temperature (July-June), then maximization occurs at lag one year (12 months) and the maximum cross correlation is 0.52. Table1 summarizes the results for all combinations examined. The lags are always positive. They have varied between 8 and 14 months for a sliding window specification and are 12 months, for the fixed window specification. Most interestingly, the opposite phase in the annual cycle of $CO_2$ concentration in the South Pole, with respect to the other three sites, does not produce any noteworthy difference in the shape of the cross-correlogram and the time lags maximizing the cross-correlations.

Table1. Maximum cross-correlation coefficient (MCCC) and corresponding time lag in months. The annual window for temperature is July-June, while for $CO_2$ it is either different (sliding), determined so as to maximize MCCC, or same (fixed).

| | Monthly time series | | Annual time series – sliding annual window | | Annual time series – fixed annual window | |
|---|---|---|---|---|---|---|
| Temperature - $CO_2$ series | MCCC | Lag | MCCC | Lag | MCCC | Lag |
| UAH – Mauna Loa | 0.47 | 5 | 0.66 | 8 | 0.52 | 12 |
| UAH – Barrow | 0.31 | 11 | 0.70 | 14 | 0.59 | 12 |
| UAH – South Pole | 0.37 | 6 | 0.54 | 10 | 0.38 | 12 |
| UAH – Global | 0.47 | 6 | 0.60 | 11 | 0.60 | 12 |
| CRUTEM4 – Mauna Loa | 0.31 | 5 | 0.55 | 10 | 0.52 | 12 |
| CRUTEM4 – Global | 0.33 | 9 | 0.55 | 12 | 0.55 | 12 |

# 5 Physical interpretation

The omnipresence of positive lags on both monthly and annual time scales reduces the likelihood that our results are statistical artefacts. Still, our results require physical interpretation which we seek in the natural process of soil respiration.

Soil respiration, $R_s$, defined to be the flux of microbially and plant-respired $CO_2$, clearly increases with temperature. It is known to have increased in the recent years (Bond-Lamberty and Thomson, 2010; IPCC, 2013). Observational data of $R_s$ (e.g. Makita et al., 2018) show that process intensity increases with temperature. Rate of chemical reactions, metabolic rate, as well as microorganism activity, generally increase with temperature. This has been known for more than 70 years and is routinely used in engineering design (Pomeroy and Bowlus, 1946).

The latest report of IPCC (IPCC, 2013, Fig. 6.1) gives quantification of the mass balance of the carbon cycle in the atmosphere, representative of the recent years. The soil respiration, assumed to be the sum of respiration (plants) and decay (microbes) is 113.7 Gt C/year (IPCC gives a value of 118.7 including fire, which, along with biomass burning, is estimated to 5 by Green and Byrne, 2004).

We can expect that the sea respiration would have increased too. Also, the photosynthesis must have been increased as in the 21st century the earth has been greening, mostly due to $CO_2$

fertilization effects (Zhu et al., 2016) and human land-use management (Chen et al., 2019). Specifically, satellite data show a net increase in leaf area of 2.3% per decade (Chen et al., 2019). The sums of carbon outflows from the atmosphere (terrestrial and maritime photosynthesis as well as maritime absorption) amount to 203 Gt C / year. The carbon inflows to the atmosphere amount to 207.4 Gt C / year and include natural terrestrial processes (respiration, decay, fire, freshwater outgassing as well as volcanism and weathering), natural maritime processes (respiration) as well as anthropogenic processes. The latter comprise human $CO_2$ emissions related to fossil fuels and cement production as well as land-use change, and amount to 7.7 Gt C / year and 1.1 Gt C / year, respectively. The change in carbon fluxes due to natural processes is likely to exceed the change due to anthropogenic $CO_2$ emissions, even though the latter are generally regarded as responsible for the imbalance of carbon in the atmosphere.

# 6 Conclusion

Relationships between atmospheric concentration of carbon dioxide and the global temperature are widely recognized and a common knowledge is that increasing $CO_2$ concentration plays the major role in enhancement of the greenhouse effect and contributes to global warming.

While the fact that these two variables are tightly connected is beyond doubt, the direction of the causal relationship needs to be studied further. The purpose of this study is to complement the conventional and established theory that increased $CO_2$ concentration due to anthropogenic emissions cause increase of temperature, by considering the concept of reverse causality. The problem is obviously more complex than that of exclusive roles of cause and effect, classifying it as a “hen-or-egg” (“ὄρνις ἢ ᾠὸν”) causality problem, where it is not always clear which of two interrelated events is the cause and which the effect. Since increased temperature causes increase in $CO_2$ concentration, hence we propose the formulation of the entire process in terms of a “hen-or-egg” causality.

We examine the relationship of global temperature and atmospheric carbon dioxide concentration using the most reliable global data that are available—the data gathered from several sources, covering the common time interval 1980-2019, available at the monthly time step.

The results of the study support the hypothesis that both causality directions exist, with the latter ($T \rightarrow CO_2$) being the dominant, despite the fact that the former ($CO_2 \rightarrow T$) prevails in public, as well as in scientific, perception. Indeed, our results show that changes in $CO_2$ follow changes in $T$ by about six months on monthly scale, or about one year on annual scale.

The opposite causality direction opens a nurturing interpretation question. We attempted to interpret this mechanism by noting the possibility of a positive feedback loop: increase of soil respiration leads to increasing $CO_2$ emission accompanying the temperature rise. We pose the challenging scientific question of interpretation for further studies whose results would, no doubt, find their way to professional literature. In our opinion, scientists of the 21st century should have been familiar with unanswered scientific questions, as well as with the idea that complex systems resist simplistic explanations.

# Appendix A. Some notes on the averaged differenced process

The cumulative process of the differenced process $\underline{\tilde{x}}_{\tau,\nu}$ will be:

$$\tilde{\underline{X}}_{\kappa,\nu} \coloneqq \tilde{\underline{x}}_{1,\nu} + \tilde{\underline{x}}_{2,\nu} + \cdots + \tilde{\underline{x}}_{\kappa,\nu} = \underline{x}_{1+\nu} - \underline{x}_1 + \underline{x}_{2+\eta} - \underline{x}_2 + \cdots + \underline{x}_{\kappa+\nu} - \underline{x}_\kappa \\ = \underline{X}_{\kappa+\nu} - \underline{X}_\nu - \underline{X}_\kappa \tag{A1}$$

Note that for $\eta$ = 1 this simplifies to

$$\tilde{\underline{X}}_{\kappa,1} = \underline{X}_{\kappa+1} - \underline{X}_1 - \underline{X}_\kappa = \underline{x}_{\kappa+1} - \underline{x}_1 = \tilde{\underline{x}}_{\kappa,1} \eqqcolon \tilde{\underline{x}}_\kappa \tag{A2}$$

Following equation (7), the average differenced process at discrete time scale $\kappa = \eta$ will be:

$$\tilde{\underline{x}}_\tau^{(\kappa)} = \frac{\tilde{\underline{X}}_{\tau\kappa,\kappa} - \tilde{\underline{X}}_{(\tau-1)\kappa,\kappa}}{\kappa} = \frac{(\underline{X}_{\tau\kappa+\kappa} - \underline{X}_\kappa - \underline{X}_{\tau\kappa}) - (\underline{X}_{(\tau-1)\kappa+\kappa} - \underline{X}_\kappa - \underline{X}_{(\tau-1)\kappa})}{\kappa} \tag{A3}$$

which, noting that in the rightmost part the two terms $\underline{X}_\kappa$ cancel each other and by virtue of (7), simplifies to:

$$\tilde{\underline{x}}_\tau^{(\kappa)} = \underline{x}_{\tau+1}^{(\kappa)} - \underline{x}_\tau^{(\kappa)} = \tilde{\underline{x}}_{\tau,1}^{(\kappa)} \tag{A4}$$

In other words, the average differenced process equals the differenced average process in case that the differencing time step $\eta$ has chosen equal to the averaging time scale $\kappa$. For $\kappa = \eta = 1$ we have $\tilde{\underline{x}}_\tau^{(1)} \equiv \tilde{\underline{x}}_{\tau,1} \equiv \tilde{\underline{x}}_\tau$.

## Appendix B. Some notes on (unidirectional) causal systems

In a unidirectional causal system in continuous time $t$, in which the process $\underline{x}(t)$ is the cause of $\underline{y}(t)$, an equation of the form:

$$\underline{y}(t) = \int_0^\infty \alpha(s)\, \underline{x}(t-s)\mathrm{d}s \tag{B1}$$

should hold (Papoulis, 1991), where $\alpha(t)$ is the impulse response function. The causality condition is:

$$\alpha(t) = 0 \text{ for } t < 0 \tag{B2}$$

Here we consider systems with positive dependence, in which $\alpha(t) \geq 0$ for $t \geq 0$, which possibly are also excited by another process $\underline{v}(t)$, independent of $\underline{x}(t)$. Working in discrete time we write:

$$\underline{y}_\tau = \sum_{j=0}^{\infty} \alpha_j\, \underline{x}_{\tau-j} + \underline{v}_\tau \tag{B3}$$

Assuming (without loss of generality) zero means for all processes, multiplying by $\underline{x}_{\tau-\eta}$, taking expected values and denoting the cross-covariance function as $c_{xy}[\eta] \coloneqq E\left[\underline{x}_{\tau-\eta}\underline{y}_\tau\right]$ and the autocovariance function as $c_x[\eta] \coloneqq E\left[\underline{x}_{\tau-\eta}\underline{x}_\tau\right]$ we find:

$$c_{xy}[\eta] = \sum_{j=0}^{\infty} \alpha_j\, c_x[\eta - j] \tag{B4}$$

For $\eta > 0$, using the property that $c_x[\eta]$ is an even function ($c_x[\eta] = c_x[-\eta]$) we get:

$$c_{xy}[\eta] = \sum_{j=0}^{\infty} \alpha_j\, c_x[j-\eta] = \sum_{j=0}^{\eta-1} \alpha_j\, c_x[\eta-j] + \sum_{j=\eta}^{\infty} \alpha_j\, c_x[j-\eta] \tag{B5}$$

and for the negative part:

$$c_{xy}[-\eta] = \sum_{j=0}^{\infty} \alpha_j\, c_x[j+\eta] \tag{B6}$$

With an intuitive reasoning, assuming that the autocovariance function is decreasing ($c_x[j'] < c_x[j]$ for $j' > j$), as usually happens in natural processes, we may see that the rightmost term of equations (B5) and (B6) should be decreasing functions of $\eta$ (as for $j' > j$ it will be $c_x[j'-\eta] < c_x[j-\eta]$ and $c_x[j'+\eta] < c_x[j+\eta]$). However, the term $\sum_{j=0}^{\eta-1} \alpha_j\, c_x[\eta-j]$ of equation (B5), is not decreasing. Therefore, it should attain a maximum value at some positive lag $\eta = \eta_1$. Thus, a positive maximizing lag, $\eta = \eta_1 > 0$, is a necessary condition for causality directional from $\underline{x}_\tau$ to $\underline{y}_\tau$. Conversely, the condition that the maximizing lag is negative is a sufficient condition to exclude the causality direction exclusively from $\underline{x}_\tau$ to $\underline{y}_\tau$.

All above arguments remain valid if we standardize (divide) by the product of standard deviations of the processes $\underline{x}_\tau$ and $\underline{y}_\tau$, and thus we can replace cross-covariances $c_{xy}[\eta]$ with cross-correlations $r_{xy}[\eta]$ (or, in the case of differenced processes, $r_{\tilde{x}\tilde{y}}[\nu, \eta]$).

## Appendix C. Graphical depictions of cross-correlograms for different combinations of temperature and carbon dioxide data

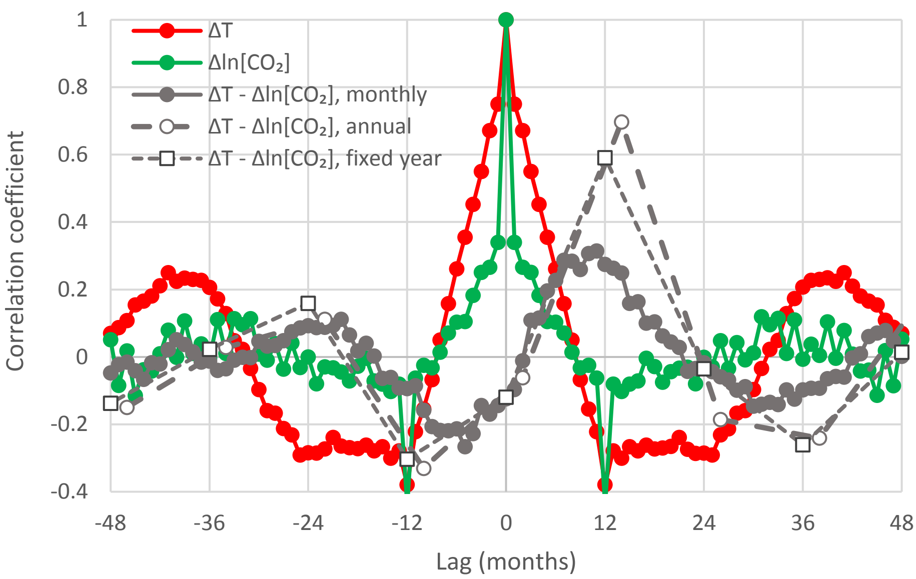


Figure C1. Auto- and cross-correlograms of the differenced time series of UAH temperature and Barrow $CO_2$ concentration.

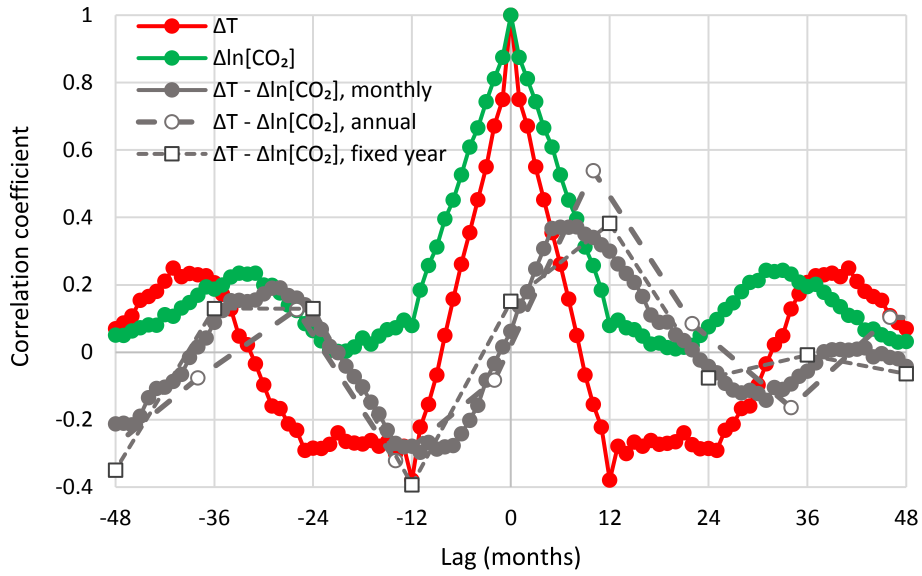


Figure C2. Auto- and cross-correlograms of the differenced time series of UAH temperature and South Pole $CO_2$ concentration.

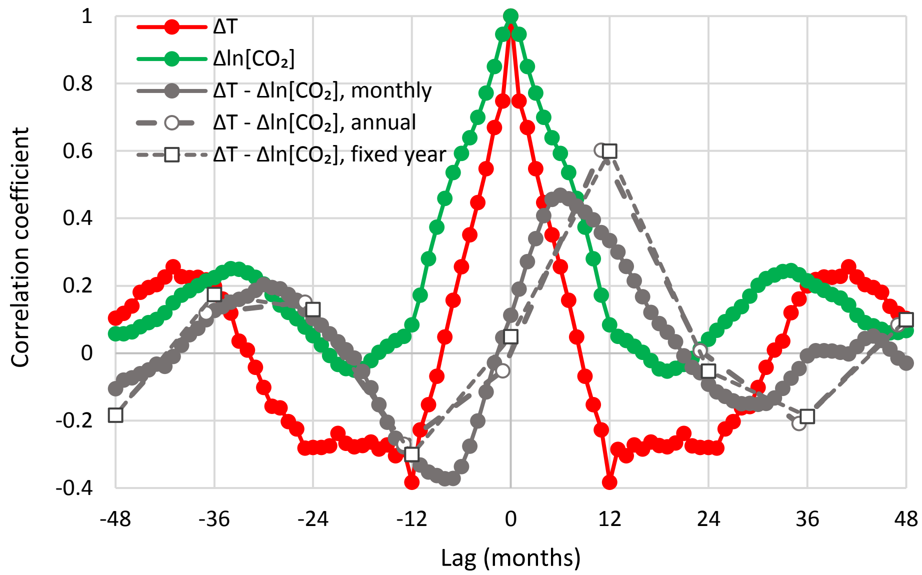


Figure C3. Auto- and cross-correlograms of the differenced time series of UAH temperature and global $CO_2$ concentration.

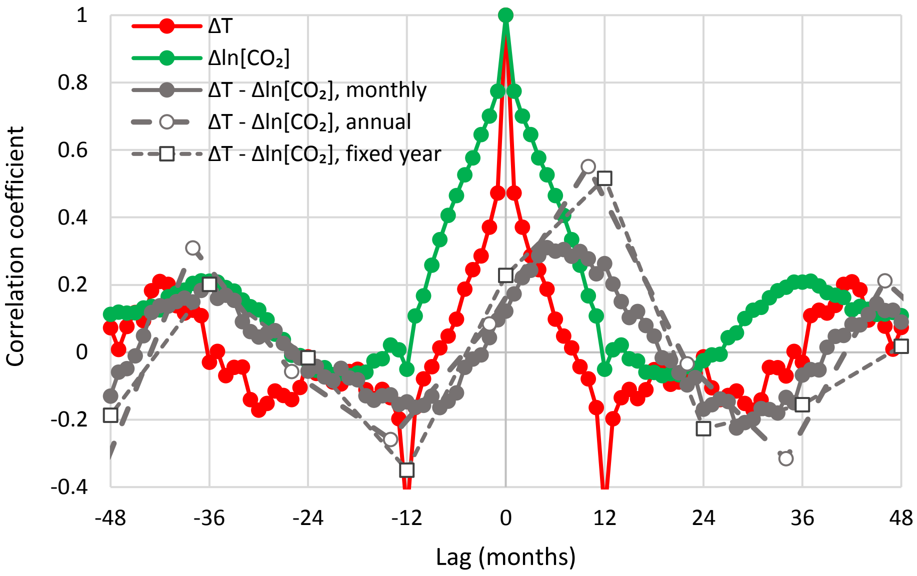


Figure C4. Auto- and cross-correlograms of the differenced time series of CRUTEM4 temperature and Mauna Loa $CO_2$ concentration.

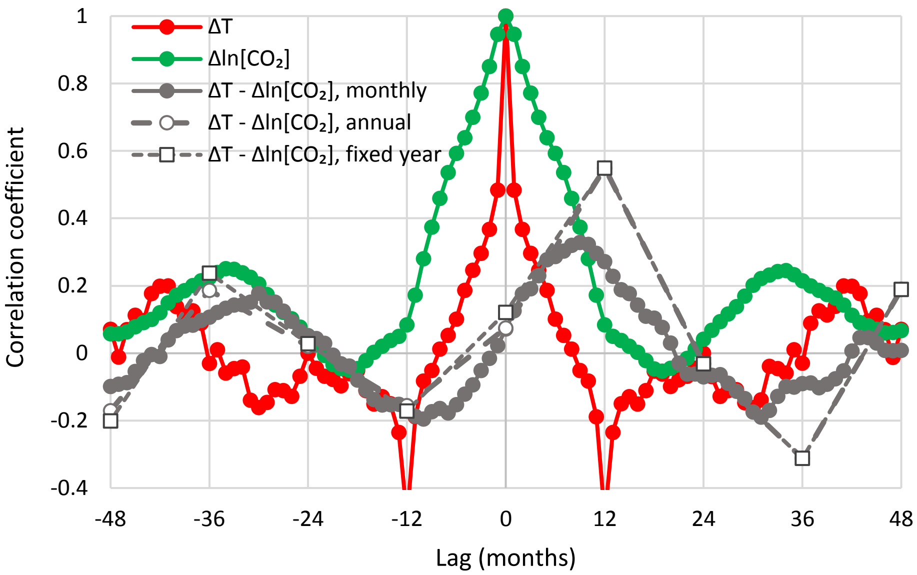


Figure C5. Auto- and cross-correlograms of the differenced time series of CRUTEM4 temperature and global $CO_2$ concentration.

## Data availability

The two temperature time series and the Mauna Loa $CO_2$ time series are readily available on monthly scale from http://climexp.knmi.nl. All NOAA $CO_2$ data are available from https://www.esrl.noaa.gov/gmd/ccgg/trends/gl_trend.html. The $CO_2$ data of Mauna Loa were retrieved from http://climexp.knmi.nl/data/imaunaloa_f.dat while the original measurements are in https://www.esrl.noaa.gov/gmd/dv/iadv/graph.php?code=MLO. The Barrow series is available (in irregular step) in https://www.esrl.noaa.gov/gmd/dv/iadv/graph.php?code=BRW, and the South Pole series in https://www.esrl.noaa.gov/gmd/dv/data/index.php?site=SPO. All these data were accessed (using the "Download data" link in the above sites) in June 2020. The global $CO_2$ series is accessed at https://www.esrl.noaa.gov/gmd/ccgg/trends/gl_data.html, of which the "Globally averaged marine surface monthly mean data" are used here.

The palaeoclimatic data of Vostok $CO_2$ were retrieved from http://cdiac.ess-dive.lbl.gov/ftp/trends/co2/vostok.icecore.co2 (dated Jan. 2003, accessed Sep. 2018) and the temperature data from http://cdiac.ess-dive.lbl.gov/ftp/trends/temp/vostok/vostok.1999.temp.dat (dated Jan. 2000, accessed Sep. 2018).

## References


Arrhenius, S., 1896. On the influence of carbonic acid in the air upon the temperature of the ground. *The London, Edinburgh, and Dublin Philosophical Magazine and Journal of Science*, 41 (251), 237-276, doi: 10.1080/14786449608620846.

Berner, R.A., 2008. Addendum to "inclusion of the weathering of volcanic rocks in the GEOCARBSULF model" (R. A. Berner, 2006, v. 306, p. 295–302). *American Journal of Science*, 308, 100–103.

Bond-Lamberty, B., and Thomson, A., 2010. Temperature-associated increases in the global soil respiration record. *Nature*, 464, 579.

Caillon, N., Severinghaus, J.P., Jouzel, J., Barnola, J.M., Kang, J. and Lipenkov, V.Y., 2003. Timing of atmospheric $CO_2$ and Antarctic temperature changes across Termination III. *Science*, 299 (5613), 1728-1731.

Chen, C., Park, T., Wang, X., Piao, S., Xu, B., Chaturvedi, R.K., Fuchs, R., Brovkin, V., Ciais, P., Fensholt, R. and Tømmervik, H., 2019. China and India lead in greening of the world through land-use management, *Nature Sustainability*, $CO_2$(2), 122-129.

Chowdhry Beeman, J., Gest, L., Parrenin, F., Raynaud, D., Fudge, T. J., Buizert, C., and Brook, E. J., 2019. Antarctic temperature and $CO_2$: near-synchrony yet variable phasing during the last deglaciation, *Clim. Past*, 15, 913–926, doi: 10.5194/cp-15-913-2019.

Christy, J.R., Norris, W.B., Spencer, R.W., and Hnilo, J.J., 2007. Tropospheric temperature change since 1979 from tropical radiosonde and satellite measurements, J*ournal of Geophysical Research*, 112, D06102, doi:10.1029/2005JD006881.

Davis, W. J., 2017. The Relationship between Atmospheric Carbon Dioxide Concentration and Global Temperature for the Last 425 Million Years. *Climate*, 5 (4), 76.

De Marchi, L., 1895. Le Cause dell'Era Glaciale. Premiato dal R. Instituto Lombardo, Pavia.

Ekart, D.D., Cerling, T.E., Montanez, I.P. and Tabor, N.J., 1999. A 400 million year carbon isotope record of pedogenic carbonate: implications for paleoatmospheric carbon dioxide. *American Journal of Science*, 299 (10), 805-827.

Granger, C.W., 1980. Testing for causality: a personal viewpoint. *Journal of Economic Dynamics and Control*, 2, 329-352.

Green, C., and Byrne, K.A., 2004. Biomass: Impact on carbon cycle and greenhouse gas emissions. *Encyclopedia of Energy*, Ed. by Cleveland, C.J. Elsevier, 223-236, doi: 10.1016/B0-12-176480-X/00418-6.

Heller, M., 1983. Time, causality, and the quantum theory. *The Review of Metaphysics*, 37 (2), 408–409.

Hurst, H.E., 1951. Long term storage capacities of reservoirs. *Trans. Am. Soc. Civil Eng.*, 116, 776–808.

IEA (International Energy Agency), 2020. Global Energy Review 2020, IEA, Paris https://www.iea.org/reports/global-energy-review-2020.

IPCC: Climate Change 2013: The Physical Science Basis. Contribution of Working Group I to the Fifth Assessment Report of the Intergovernmental Panel on Climate Change. Cambridge University Press, Cambridge, UK and New York, NY, 1535 pp. http://www.climatechange2013.org/report/ (accessed 2020-02-14), 2013.

Jones, P.D., Lister, D.H., Osborn, T.J., Harpham, C., Salmon, M., and Morice C.P., 2012. Hemispheric and large-scale land surface air temperature variations: An extensive revision and an update to 2010. *J. Geophys. Res.*, 117, D05127, doi: 10.1029/2011JD017139.

Jouzel, J., Lorius, C., Petit, J.R., Genthon, C., Barkov, N.I., Kotlyakov, V.M., and Petrov, V.M., 1987. Vostok ice core: a continuous isotope temperature record over the last climatic cycle (160 000 years). *Nature*, 329, 403-408.

Keeling, C.D., Bacastow, R.B., Bainbridge, A.E., Ekdahl, C.A., Guenther, P.R., and Waterman, L.S., 1976. Atmospheric carbon dioxide variations at Mauna Loa Observatory, Hawaii. *Tellus*, 28, 538-551.

Kline, A.D., 1980. Are there cases of simultaneous causation?. In PSA: *Proceedings of the Biennial Meeting of the Philosophy of Science Association*, Vol. 1980, 1, 292-301, Philosophy of Science Association.

Kolmogorov, A.N., 1940. Wienersche Spiralen und einige andere interessante Kurven im Hilbertschen Raum. Dokl. Akad. Nauk SSSR, 26, 115–118. (English edition: Kolmogorov, A.N., 1991. Wiener spirals and some other interesting curves in a Hilbert space. Selected Works of A. N. Kolmogorov - Volume 1, Mathematics and Mechanics, Tikhomirov, V. M. ed., Kluwer, Dordrecht, The Netherlands, pp. 303-307).

Koutsoyiannis, D., 2016. Generic and parsimonious stochastic modelling for hydrology and beyond. *Hydrological Sciences Journal*, 61 (2), 225–244, doi: 10.1080/02626667.2015.1016950.

Koutsoyiannis, D., 2019. Time's arrow in stochastic characterization and simulation of atmospheric and hydrological processes. *Hydrological Sciences Journal*, 64 (9), 1013–1037, doi: 10.1080/02626667.2019.1600700.

Koutsoyiannis, D., 2020. Revisiting global hydrological cycle: Is it intensifying?. *Hydrology and Earth System Sciences*, doi: 10.5194/hess-2020-120.

Kundzewicz, Z.W., Pińskwar, I., Koutsoyiannis, D., 2020. Variability of global mean annual temperature is significantly influenced by the rhythm of ocean-atmosphere oscillations. *Science of the Total Environment* (revised, in review)

Lawrance, A.J., 1991. Directionality and reversibility in time series. *International Statistical Review*, 59 (1) 67-79.

Makita, N., Kosugi, Y., Sakabe, A., Kanazawa, A., Ohkubo, S., Tani, M., 2018. Seasonal and diurnal patterns of soil respiration in an evergreen coniferous forest: Evidence from six years of observation with automatic chambers. *PLoS One* 13 (2), e0192622, doi: 10.1371/journal.pone.0192622.

Papoulis, A., 1991. *Probability, Random Variables and Stochastic Processes*, 3rd edn. McGraw-Hill, New York.

Pedro, J.B., Rasmussen, S.O. and van Ommen, T.D., 2012. Tightened constraints on the time-lag between Antarctic temperature and $CO_2$ during the last deglaciation. *Climate of the Past*, 8(4), 1213-1221.

Peters, G.P., Marland, G., Le Quéré, C., Boden, T., Canadell, J.G., Raupach, M.R., 2012. Rapid growth in $CO_2$ emissions after the 2008-2009 global financial crisis. *Nat. Clim. Chang.,* 2, 2–4, doi: 10.1038/nclimate1332.

Petit, J.R., Jouzel, J., Raynaud, D., Barkov, N.I., Barnola, J.-M., Basile, I., Bender, M., Chappellaz, J., Davis, M., Delayque, G., Delmotte, M., Kotlyakov, V.M., Legrand, M., Lipenkov, V.Y., Lorius, C., Pepin, L., Ritz, C., Saltzman, E., and Stievenard. M., 1999. Climate and atmospheric history of the past 420,000 years from the Vostok ice core, Antarctica. *Nature*, 399, 429-436.

Pomeroy, R. and Bowlus, F.D., 1946. Progress report on sulfide control research. *Sewage Works Journal*, 18 (4), 597-640.

Roe, G., 2006. In defense of Milankovitch. *Geophysical Research Letters*, 33(24), 10.1029/2006GL027817

Schmidt, G.A., Ruedy, R.A., Miller, R.L., and Lacis, A.A., 2010. Attribution of the present-day total greenhouse effect. *J. Geophys. Res.*, 115, D20106, doi:10.1029/2010JD014287.

Soon, W., 2007. Implications of the secondary role of carbon dioxide and methane forcing in climate change: past, present, and future. *Physical Geography*, 28(2), 97-125.

Spencer, R.W. and Christy, J.R., 1990. Precise monitoring of global temperature trends from satellites. *Science*, 247 (4950), 1558-1562.

Suppes, P., 1970. *A Probabilistic Theory of Causality*. North-Holland Publishing, Amsterdam.

Tong, H. and Zhang, Z., 2005. On time-reversibility of multivariate linear processes. *Statistica Sinica*, 15(2), 495-504.

Veizer, J., et al., 2000. 87Sr/86Sr, d13C and d18O evolution of Phanerozoic seawater. *Chem. Geol.*, 161, 59-88.

Weiss, G., 1975. Time-reversibility of linear stochastic processes. *Journal of Applied Probability*, 12(4), 831-836.

Zhu, Z., Piao, S., Myneni, R.B., Huang, M., Zeng, Z., Canadell, J.G., Ciais, P., Sitch, S., Friedlingstein, P., Arneth, A. and Cao, C,. 2016. Greening of the Earth and its drivers, *Nature Climate Change*, 6 (8), 791-795.